
Article:
Wang, L, Sun, Y, Wignall, PB orcid.org/0000-0003-0074-9129 et al. (3 more authors) (2023) The Permian-Triassic Merrillina (conodont) in South China and its ecological significance. Marine Micropaleontology, 180. 102228. ISSN 0377-8398

https://doi.org/10.1016/j.marmicro.2023.102228

The Permian-Triassic *Merrillina* (conodont) in South China and its ecological significance

Lina Wang*[1,2], Yadong Sun*[3], Paul B. Wignall[4], Anna Xing[5], Zongxia Chen[1,2], Xulong Lai[3]

1. Hebei Key Laboratory of Strategic Critical Mineral Resources, Hebei GEO University, Shijiazhuang, Hebei 050031, People's Republic of China
2. School of Earth Science, Hebei GEO University, Shijiazhuang, Hebei 050031, People's Republic of China
3. State Key Laboratory of Biogeology and Environmental Geology, China University of Geosciences (Wuhan), Wuhan 430074, People's Republic of China
4. School of Earth and Environment, University of Leeds, Leeds LS2 9JT, UK
5. Department of Resources and Environment, Huaxin College of Hebei GEO University, Xinle, Hebei 050700, People's Republic of China

*Corresponding author: Lina WANG (wanglina0605@163.com); Yadong SUN (yadong.sun@cug.edu.cn)

Abstract:

Conodonts from Permian-Triassic Boundary (P-TB) beds have been intensively investigated in recent years. Many species survived the end-Permian mass extinction, and some became cosmopolitan in the earliest Triassic. Most studies have focused on common families such as the Gondolellidae and the Achignathodidae, whilst the Ellisonidae is understudied due to the difficulties of reconstructing their multi-element apparatus. Here, we focus on the Ellisonidae from the Meishan, Shangsi and Gaohua sections in South China and find *Merrilina* (*M.*) spp. are common taxa. A representative species, *M. ultima*, previously regarded as a Changhsingian cool-water species, is found in warm, shallow platform settings of the earliest Triassic. Biostratigraphically, *M. ultima* ranges from the *Hindeodus parvus* Zone to the *Isarcicella staeschei* Zone at Meishan and to the *I. isarcica* Zone at Gaohua, whilst it only occurred in the *Clarkina taylore* Zone at Shangsi. A compilation of all published data suggests *M. ultima* firstly appeared in the *C. meishanensis-H. praeparvus* Zone and went extinct in the *I. isarcica* Zone. *Merrillina* spp. occur in various settings and latitudes, indicating that the species were likely cosmopolitan taxa that favoured surface-water habitats and were not restricted to cool waters.

Key Words: *Merrillina*, Ellisonidae, Permian-Triassic Boundary, Meishan section, Shangsi section

1. Introduction

The largest mass extinction of the Phanerozoic occurred in the latest Permian and eliminated nearly 80% of marine species (Fan et al., 2020). The ultimate cause(s) of the end-Permian Mass Extinction (EPME) is intensely debated, probably involving multiple killing mechanisms such as ocean deoxygenation, ocean acidification, and climate warming linked to the Siberian Traps eruption (Wignall and Hallam, 1992; Sun et al., 2012; Bond and Wignall, 2014; Burgess and Bowring, 2015; Clarkson et al., 2015; Benton, 2018). The aftermath of the EPME was characterised by persistent environmental stress that delayed the full recovery of the ecosystem (Bottjer, 2004; Payne et al., 2004; Sun et al., 2012). A minor late Early Triassic radiation began around 249.58 Ma, but marine diversity remained low until the early Middle Triassic (Fan et al., 2020).

Compared with most marine taxa, conodonts suffered only modest losses during the EPME and remained relatively diverse throughout the Early Triassic (Orchard, 2007). A handful of species went extinct, but these were not substantially higher losses than those seen during background turnover. Four families, namely Achignathodontidae Clark 1972, Gondolellidae Lindström 1970, Ellisonidae Clark 1972, and Vjalovognathidae Shen, Yuan & Henderson 2015 are known from Permian-Triassic boundary (P-TB) beds. Only the Vjalovognathidae went extinct during the EPME.

In the aftermath of the end-Permian mass extinction, many surviving species expanded their geographic and ecological ranges, becoming cosmopolitan in the Early Triassic. The genera *Hindeodus*, *Isarcicella*, *Clarkina*, *Neogondolella*, *Stepanovites*, *Merrillina*, *Hadrodontina*, *Pachycladina*, and *Ellisonia* were globally widespread (Jin et al., 1996; Orchard and Krystyn, 1998; Wardlaw and Mei, 1999; Shen et al., 2006; Jiang et al., 2007; Kozur, 2007; Wang et al., 2017; Sun et al., 2021). *Hindeodus* and *Isarcicella* belong to the Achignathodontidae; *Clarkina*, *Neogondolella*, *Mesogondolella* belong to the Gondolellidae. The Ellisonidae clan includes common

genera such as *Stepanovites*, *Merrillina*, *Hadrodontina*, *Pachycladina*, and *Ellisonia.* The Vjalovognathidae contains only one genus — *Vjalovognathus*. *Mesogondolella* and *Vjalovognathus* have a restricted distribution, occurring sparsely in the Perigondowana region (Brookfield and Sun, 2015; Wang et al., 2017).

Most P-TB conodont studies have focused on the taxonomy and biostratigraphy of the Achignathodontidae and the Gondolellidae (Zhang et al., 1995; Metcalfe et al., 2011; Yan et al., 2013), whilst only a few studies have examined the Early Triassic Ellisonidae (Koike et al., 2004; Koike, 2016). In this study, we provide a comprehensive study of the Ellisonidae in South China, including a detailed taxonomic description of representative taxa, and reveal their spatiotemporal distribution in P-TB strata.

2. Studied sections and materials

Three P-TB sites in South China were investigated: Meishan (Zhejiang Province), Shangsi (Sichuan Province), and Gaohua (Hunan Province). The sections were located either in slope settings developed adjacent to the Yangtze carbonate platform or on the platform (Fig. 1). The Meishan section is the Global Stratotype Section and Point (GSSP) for the P-TB and has been intensively studied (e.g., Yin et al., 2001, 2014; Shen, 2012). The P-TB strata are composed of the Changxing Formation and the Yinkeng Formation, which were deposited in an upper slope setting. The Changxing Formation spans the uppermost Wuchiapingian to the Changhsingian, and is characterised by micrite and thinly interbedded chert horizons. The Griesbachian Yinkeng Formation mainly consists of shales and marls with minor, thin-bedded, micritic limestones (Yang and Jiang, 1981; Zhang and Tong, 1996). The Shangsi section consists of the upper Permian Talung Formation and the lower Triassic Feixianguan Formation, which record deposition in lower slope and intra-platform basin settings. The Talung Formation consists of bedded cherts, cherty carbonates, marl and thin shales. The Feixianguan Formation consists mainly of thin-bedded, micritic and argillaceous limestones (Li et

al., 1989). The Gaohua section is composed of bioclastic micrites of the uppermost Changxing Formation and microbial and micritic limestones interbedded with ooids limestones of the Daye Formation. The section represents a shallow-water carbonate platform setting (Wang et al., 2016).

A total of 47 samples, weighing 2-6 kg, were collected from the three study sections. Samples were dissolved in dilute acetic acid (~8 %), wet sieved, and dried at room temperature. A heavy sodium polytungstate liquid (2.81 g/ml) was used to separate heavy fractions. *Merrilina* spp. were selected from conodont assemblages for this study. Data from published studies (e.g., Jiang et al., 2014; Wang et al. 2017) are compiled for quantitative comparisons with *Clarkina*, *Hindeodus* and *Isarcicella*.

3. Results

Although rare, all study sections yielded *Merrillina*. Taxonomically, *Merrillina* has much more robust elements than *Hindeodus* and *Isarcicella* and can be easily differentiated from the ramiform elements of *Clarkina*.

3.1 The Meishan section

A total of 31 *Merrillina ultima* specimens were recovered from beds 27c and 28 in the Meishan section (Table 2, Fig. 2-3). These include P_1, P_2, S_1, S_2, $S_{3/4}$, and M elements. One P_1 element (Fig. 2.1) and one $S_{3/4}$ element (Fig. 3.1) were found in Bed 27c, which belongs to the base of the *H. parvus* Zone (Fig. 4). They co-occur with *Clarkina carinata*, *C. changxingensis*, *C. deflecta*, *C. tulongensis*, *C. zhejiangensis*, *C. meishanensis*, *C. taylorae*, *C. planata*, *H. typicalis*, *H. praeparvus*, *H. pisai*, *H. changxingensis*, *H. eurypyge*, and *H. parvus*. More P_1 (Fig. 2. 3-2.6, 2.9), P_2 (Fig. 2.2), S_1 (Fig. 2.8; Fig. 3.4, 3.5? 3.9, 3.11-3.12), S_2 (Fig. 2.7; Fig. 3.8, 3.10), $S_{3/4}$ (Fig. 3.2-3.3), and M (Fig. 3.6-3.7) elements were recovered in Bed 28 of the *I. staeschei* Zone (Fig. 4). They co-occur with *C. carinata*, *C. changxingensis*, *C. deflecta*, *C. tulongensis*, *C.*

zhejiangensis, *C. meishanensis*, *C. taylorae*, *C. planata*, *H. typicalis*, *H. praeparvus*, *H. pisai*, *H. changxingensis*, *H. eurypyge*, *H. parvus*, *I. staeschei*, *I. lobata,* and *I. peculiaris*.

3.2 The Shangsi section

Three *M. ultima* specimens were found in the Shangsi section (Table 2). One each of P_1 (Fig. 5.2), M (Fig. 5.1) and $S_{3/4}$ (Fig. 5.3) elements were recovered in Bed 28b of the Feixianguan Formation, which was in the lower part of the *H. changxingensis* Zone (Fig. 4). Their associated taxa are *H. changxingensis*, *C. deflecta*, *C. taylorae*, *I. huckriedei*, *I. prisca*, *H. praeparvus*, *C. carinata*, *I. turgida*, and *H. eurypyge*. Although the FAD of *H. parvus* is not established at Shangsi, the P-TB is placed in the middle of Bed 28a based on other criteria (Jiang et al., 2011; Yin et al., 2014). Hence, *M. ultima* appears at the base of the Griesbachian at this location.

3.3 The Gaohua section

In the Gaohua section, a single P_1 (Table 2; Fig. 5.4), P_2 (Fig. 5.5), $S_{3/4}$ (Fig. 5.6), and S_1 element were found in the lower part of the microbialite unit of the basal Daye Formation, corresponding to the *H. parvus* Zone. They are associated with *H. praeparvus*, *H. parvus*, *H. typicalis*, and *H. bicuspidatus*. Two $S_{3/4}$ (Fig. 5.7) and two M elements were recovered in the ooid beds of the Daye Formation, which belong to the *I. isarcica* Zone. At this level, *M. ultima* co-occurs with *H. praeparvus*, *H. parvus*, *H. typicalis*, *I. staschei*, *I. isarcica* and *I. turgida*. No S_0 element is found.

3.4 Rarity of *Merrillina* in the P-TB of South China

Merrillina (P_1) is rare in study sections compared to other conodont taxa. As shown in Table 1, 70.33% of the P_1 elements are *Clarkina*, 29.65% are *Hindeodus-*

Isarcicella (P_1), and only 0.02% are *Merrillina* at Meishan. Similarly, at Shangsi, 56.76% of all conodont species are *Clarkina*, whereas 43.20% of taxa belong to *Hindeodus* and *Isarcicella* (P_1), and only 0.41% are *Merrillina*. In the shallow water Gaohua section, *Hindeodus* and *Isarcicella* are dominant, comprising 98.55% of all P_1 elements. *Clarkina* and *Merrillina* are both low in abundance, occupying only 0.72% of the assemblage.

4. Systematic paleontology

Genus *Merrillina* KOZUR, 1975

Type species: *Spathognathodus divergens* BENDER & STOPPEL, 1965

Merrillina ultima Kozur, 2004

Fig. 2-3; 5

2004 *M. ultima* -Kozur, 2004, page 5, figs.15-16 Plate 1

2004 *Stepanovites? mostleri* -Kozur, 2004, page 57, figs.27-29 Plate 1

2015 *M. ultima*-Wardlaw et al., 2015, pages 327, 331, figs.5,9 Plate 4; figs. 1-13, Plate 6

Diagnosis: the breviform digyrate P_1 element is small and has a distinct cusp, with two to five discrete denticles located on the relatively low blade. The angulate digyrate P_2 element is twisted distinctly. The digyrate M element has an obvious cusp and curves inwardly. The alate S_0 element is triramous, inclines posteriorly and has a large ultimate denticle. The strongly arched S_1 element is downward curved at the posterior end. The S_2 element is bipennate with a distinct cusp located near the middle part of the process. The bipennate S_3 and S_4 elements are similar in morphology and generally straight. The

anterior process is moderately curved inward.

Description: the P_1 element is breviform digyrate and has a distinct cusp inclined forward at ~45-50°, two-four discrete denticles on the blade, with (occasionally) a tiny denticle in front of the cusp. The denticles between the cusp and the last erect denticle are generally incline posteriorly. The lower side is moderately excavated and asymmetrical.

The twisted P_2 element is breviform digyrate and has a short anterior and a relatively longer posterior process. The cusp is quite large, and one or two smaller, near-erect denticles are located on the anterior process. Four smaller denticles incline posteriorly, sitting on the posterior process. The lower side of the element is widely excavated and is flattened in most areas of the element.

The M element is breviform digyrate and has a distinct cusp that is curved inward. The posterior process is short and bears small denticles. The anterior process bears from two to four large erect or slightly forward-inclined denticles. The lower side shows shallow excavation and is broad in both processes. A deep basal furrow is present in the central part of the element, which is rather broad in the anterior process. The basal furrow under the cusp is widened to an elongated basal cavity. The inner side of the basal cavity is widened and like an upside-down cup.

The S_0 element is alate and triramous. The elongated and slightly curved posterior process bears five to six big denticles that incline increasingly toward the posterior. The largest denticle is located in the posterior third of the posterior process. The large ultimate denticle lies in the prolongation of the posterior process and is inclined strongly. Two anterior processes are short and slightly forward-directed. A basal cavity is developed under the cusp, and the lower side under the anterior half of the posterior process is wide and deeply excavated.

The S_1 element is bipennate, slightly curved or nearly straight. A moderate cusp lies in the middle of the element and is strongly bent backwards. The anterior and

posterior processes both bear from five to seven small denticles. All the denticles are inclined backwards. Those on the anterior process vary in size, and the first denticle is nearly directed downward. Denticles on the posterior process increase in size and become more reclined posteriorly. The basal furrow is broad on the lower side and is distinctly widened below the cusp to an elongated basal cavity.

The S_2 element is bipennate, with a distinct cusp posteriorly inclined located near the middle part of the process. The posterior process beside the cusp is nearly perpendicular to the anterior process. The anterior and posterior processes are both denticulated with discrete small denticles.

The $S_{3/4}$ elements are bipennate and straight. A downward inflexion occurs at the end of the posterior process; at the anterior end, an upward inflexion appears. The anterior process is short and moderately inwardly curved at the end. It bears from one to five denticles—the first two are large. A very big cusp is inclined posteriorly. The posterior process is relatively long and bears more denticles than the anterior process, with the last two being distinctly larger and inclining posteriorly. Sometimes, a tiny denticle presents between the large denticle and the cusp. A very small denticle may occur at the posterior end of the process. The lower side is wide and deeply excavated.

Remarks: *Merrillina* is characterised by its digyrate P elements and very robust M and S elements with tall and robust cusps. Different species of *Merrillina* have distinct P_1 elements, while their S and M elements are generally similar. The *Merrillina* multi-elements generally have denticles with round cross-sections, which differ from ramiforms of other groups such as Achignathodontidae and Gondolellidae. Another Permian ellisonid, *Stepanovites* (synonymised with *Sweetina* and *Kamagnathus*), has three processes in the P_1 element. This is very different to the digyrate P_1 element in *Merrillina*. Both *Merrillina* and *Stepanovites* have M elements with an enlarged basal cavity directed to the posterior.

The P elements of *M. ultima* are breviform digyrate, the P_1 element has a very large

cusp that is posteriorly inclined. The P_2 elements are angulate twisted with distinct cusp. The M elements are breviform digyrate. The cusp is robust, tall and located in the middle part of the element. The S_0 elements are alate and triramous, the $S_{1/2}$ elements are extensiform digyrate and strongly curved. The $S_{3/4}$ elements are bipennate, straight and nearly similar in morphology.

Occurrence: *H. parvus* Zone to *I. staeschei* Zone in the Meishan section, *H. changxingensis* to *C. taylorae* Zone in the Shangsi section, *H. parvus* Zone to *I. isarcica* Zone in the Gaohua section. The uppermost Changxingian to the base of the Griesbachian.

5. Discussion

5.1 The temporal-spatial distribution of *Merrillina ultima*

M. ultima is well known in P-TB beds, e.g. in Vietnam (Wardlaw et al., 2015), South China (Metcalfe and Nicoll, 2007; Chen and Wang, 2009; Wang et al., 2016) and Iran (Kozur, 2004, 2007). In Vietnam, the P_1 element of *M. ultima* co-occurs with *H. parvus erectus* in the *H. parvus* Zone and other elements are found in the older *H. praeparvus* Zone (Wardlaw et al., 2015). In South China, *M. ultima* co-occurs with *H. praeparvus* and *C. meishanensis* in the P-TB beds at Zhongzhai, Guizhou Province (Metcalfe and Nicoll, 2007). It is also reported from microbial limestone belonging to the *C. zhejiangensis-H. eurypyge* "partial range biozone" at Dawen, which could correlate with the *C. meishanensis-H. praeparvus* Zone at Meishan (Chen et al., 2009). In the Wuzhuan section, *M. ultima* is present above the *H. parvus* Zone (Brosse et al., 2015). In Iran, *M. ultima* is recorded from the *C. meishanensis-H. praeparvus* Zone in the latest Changhsingian (Kozur, 2004).

In this study, *M. ultima* is recovered in the *C. taylorae* Zone of the Early Triassic in the Shangsi section (Jiang et al., 2011) and in the *H. parvus* Zone and the *I. staeschei* Zone in the Meishan section (Jiang et al., 2007). Most specimens from the Gaohua

section are found in the *H. parvus* Zone and the *I. isarcica* Zone.

Collectively, the first appearance of *M. ultima* is in the latest Changhsingian *C. meishanensis-H. praeparvus* Zone, an event that is synchronous in North America, Iran, and South China (Fig. 6). This short-lived species has its last occurrence in the *I. isarcica* Zone.

5.2 The ecology of *Merrillina*

M. ultima was long postulated as a cool water species of the latest Permian, and was previously only reported from Iran and North America (Mei and Henderson, 2001; Kozur, 2004, 2007). However, this notion was based on the idea that the Changhsingian to mid-Griesbachian was a cool period (Mei and Henderson, 2001). Both Iran and South China were situated in equatorial latitudes during the P-T transition and saw a seawater temperature increase of ~8-10 ºC to 38-40 ºC (Joachimski et al., 2012; Sun et al., 2012; Schobben et al., 2014). The nearly contemporaneous occurrences of *M. ultima* in the equatorial Tethyan ocean suggest the taxon was well-adapted to warm environments. Although rare, occurrences of *Merrillina* spp. in different settings and latitudes indicate that the species were cosmopolitan and likely tolerant of a broad range of temperatures (Fig. 7).

The distribution of *Merrillina* in our study sections adds further light on the environmental context (Fig. 8). In the Shangsi section, *M. ultima* was found in the lower part of the *H. changxingensis* Zone when depositional conditions were well-oxygenated (Bond and Wignall, 2010). However, in the upper part of the *C. taylorae* Zone, an anoxic event occurred in this area (Xiang et al., 2016), and no *Merrillina* is found at this level. In the Meishan section, *M. ultima* occurs in upper dysoxic-oxic facies that developed after an anoxic interval at the P-TB (Li et al., 2015). Intense anoxia develops again in the upper part of the *I. isarcica* Zone at Meishan, but *M. ultima* had already gone extinct by this level. In the Gaohua section, the species occurs in shallow-water,

upper dysoxic sediments on a carbonate platform (Wang et al., 2016). The cross-comparison of *Merrillina*'s occurrences and redox conditions recorded in its host rock reveals that the taxon only occurred in settings with Eh (redox potential) better than upper dysoxic and was also possibly a surface dweller.

5.3 Evolution of Permian-Triassic *Merrillina*

Kozur (1975) established *Merrillina* with *M. divergens* Kozur, 1975 being the type species. The genus is one of the key biostratigraphically important taxa in the Permian. *Merrillina* has several representative species. However, their evolutionary lineages are poorly understood. The oldest *Merrillina* is the Wordian *Merrillina galeata* Bender and Stoppel 1965 (Fig. 6) from Wyoming and Nevada, USA (Clark and Behnken, 1971; Wardlaw and Collinson, 1984) and Sicily (Bender and Stoppel, 1965). The P_1 element of *Merrllina galeata* is slightly twisted, and is characterised by its posteriorly direct cusp that was flanked with two subequal sized denticles anteriorly and one to four smaller denticles posteriorly.

M. galeata was succeeded by *M. divergens* of Capitanian to Wuchiapingian in ages (Fig. 7). The Capitanian *M. divergens* is widely reported from Germany (Bender and Stoppel, 1965; Swift, 1986), Poland (Szaniawski, 1969), Iran (Kozur, 2004), and North America (Wardlaw and Collinson, 1979; Wardlaw and Collinson, 1986; Wardlaw and Mei, 1998). The P_1 element of *M. divergens* is short and shows slight lateral bowing, with three to seven denticles on a mid-height blade. The denticles increased in size and inclination posteriorly. The terminal main denticle is the largest one and is sometimes succeeded by a small denticle. The basal cavity is expanded laterally, broadly flaring beneath the main denticle and tapering anteriorly. The report of *M. divergens* from Iran and in the Zechstein in the north England mark their youngest occurrence in the Late Permian (Swift and Aldridge, 1982; Swift, 1986; Kozur, 2004). *M. praedivergens* of the Capitanian age, (Clark and Behnken, 1971) was thought to be a transitional species

from *M. galeate* to *M. divergens*, which was later designated to *M. divergens* in Wardlaw et al., (2015). The specimen has fewer denticles on the carina, but a very robust cusp generally succeeded by a small anterior denticle. The denticles are more discrete compared to *M. galeata* but more fused compared to *M. divergens* (Fig. 6).

The lower Wuchiapingian *M. postdivergens* (Fig. 6; Fig. 7) is known in the northwestern Iran, ranging from the *C. asymmetrica* Zone (≈*C. niuzhuangensis* Zone) to the *C. leveni* Zone (Kozur, 2004). The P_1 element of *M. postdivergens* has a large, strongly inclined cusp, with narrow, needle-like denticles strongly inclined posteriorly, sometimes bearing a small, erect anterior denticle. Compared to *M. divergens*, *M. postdivergens* generally has fewer denticles on the carina, the strongly inclined cusp become more distinctive. The denticles of *M. postdivergens* are more discrete than those on *M. divergens* (Fig. 6).

M. ultima appeared in the latest Permian and ranged to the earliest Triassic *I. isarcica* Zone. An unidentified species of *M*. sp. (Fig. 7) has been reported from the Griesbachian at Dajiang, Guizhou Province, and could be the youngest species of this genus (Jiang et al., 2014). Although *Merrillina* was not documented in much of the upper Wuchiapingian to the lower Changshingian, other species may have existed at this time. It seems that *Merrillina* evolved larger cusps through time. The cusp of *M. ultima* are clearly more robust than those of its ancestor *M. postdivergens.* The youngest *M.* sp. from Dajiang has the most robust cusp among all known species in the genus *Merrillina* (Fig. 7).

In summary, the *Merrillina* lineage was never particularly diverse, with no more than two species extant from its first occurrence in the Wordian until its extinction in the late Griesbachian. It is noteworthy that a long evolutionary gap of ~5 Myr between *M. ultima* and *M. postdivergens* occurred in the Late Permian could be due to low research intensity (Fig. 6).

6. Conclusions

A systematic investigation of the P-TB *Merrillina* has been carried out in three sections in South China. By compiling published records of *Merrillina*, the following conclusion can be drawn:

1) *Merrillina* is an uncommon but widespread conodont genus, ranging from the Middle Permian to the earliest Triassic, that survived the vicissitudes of the Permo-Triassic boundary for a short interval. The final species, *M. ultima* was the most geographically widespread and had a near-cosmopolitan distribution.

2) *M. ultima* first appeared in the *C. meishanensis-H. praeparvus* Zone and went extinct in the *I. isarcica* Zone. The report of *M. ultima* in the Early Triassic from South China indicates that it was well-adapted to warm environments. The facies distribution of this youngest species, notably its absence from anoxic-euxinic strata, suggests that *Merrillina* probably favoured well-ventilated surface-water habits.

Acknowledgements

The authors thank Maria Cristina Perri for her guidance on the taxonomy of *Merrillina*. We are in debt to editor Dr. Xavier Crosta, Tea Kolar-Jurkovšek and one anonymous reviewer for their constructive comments. The Natural Science Foundation of China financially supported this work (grant no.: 41802016;42272022; 41821001), the Natural Science Foundation of Hebei Province, China (grant no.: D2018403044), and the PhD. Research Startup Foundation of Hebei GEO University (Grant no. BQ2017014), and the state-level top undergraduate courses of the Ministry of Education of the People's Republic of China for Petrology of sedimentary rocks [2020130286 letters no. 2020(8); 2020GJJG589; KCJSX2021092; letter no. 2021(62)].

Figure and Table captions

Fig. 1 Location map of the Meishan, Shangsi and Gaohua sections (A) and palaeogeographic reconstruction of the South China Block during the Permian-Triassic transition showing three study sections (B), revised from Yin et al., (2014).

Fig. 2 SEM photos showing *M. ultima* specimens from the Meishan section

1, 3-6, 9. *Merrillina ultima* Kozur, P_1 element, 1a, lateral view, MS 27c-i005, 1b, lower view, MS B27c-B-i005, Yinkeng Formation, sample MS B27c, *H. parvus* Zone, the base of Griesbachian; 3a, lateral view, MS B28-i033, 3b, lower view, MS B28-B-i033, Yinkeng Formation, sample MS B28, *I. staeschei* Zone, the base of Griesbachian; 4a, lateral view, MS B28-i037, 4b, lower view, MS B28-B-i037, Yinkeng Formation, sample MS B28, *I. staeschei* Zone, the base of Griesbachian; 5, lateral view, MS B28-i028, Yinkeng Formation, sample MS B28, *I. staeschei* Zone, the base of Griesbachian; 6a, lateral view, MS B28-i035, 6b, lower view, MS B28-B-i035, Yinkeng Formation, sample MS B28, *I. staeschei* Zone, the base of Griesbachian; 9, lateral view, MS B28-i027 , Yinkeng Formation, sample MS B28, *I. staeschei* Zone, the base of Griesbachian.

2. *Merrillina ultima* Kozur, P_2 element, lateral view, MS B28-i041, Yinkeng Formation, sample MS B28, *I. staeschei* Zone, the base of Griesbachian;

7. *Merrillina ultima* Kozur, S_2 element, 7a, lateral view, MS B28-i024, 7b, lower view, MS B28-B-i024, Yinkeng Formation, sample MS B28, *I. staeschei* Zone, the base of Griesbachian.

8. *Merrillina ultima* Kozur, S_1 element,8a, lateral view, MS B28-i022, 8b, lower view, MS B28-B-i022, Yinkeng Formation, sample MS B28, *I. staeschei* Zone, the base of Griesbachian.

Fig. 3 SEM photos showing *M. ultima* specimens from the Meishan section (continued)

1-3. *Merrillina ultima* Kozur, $S_{3/4}$ element, 1a, lateral view, MS 27c-i003, 1b, lower view, MS B27c-B-i003, Yinkeng Formation, sample MS B27c, *H. parvus* Zone, the base of Griesbachian; 2, lateral view, MS B28-i031, Yinkeng Formation, sample MS B28, *I. staeschei* Zone, the base of Griesbachian; 3a, lateral view, MS B28-i019, 3b, lower view, MS B28-B-i019, Yinkeng Formation, sample MS B28, *I. staeschei* Zone, the base of Griesbachian.

4,9, 11-12. *Merrillina ultima* Kozur, S_1 element, 4a, lateral view, MS B28-i021, 4b, lower view, MS B28-B-i021, Yinkeng Formation, sample MS B28, *I. staeschei* Zone, the base of Griesbachian; 9a, lateral view, MS B28-i021, 9b, lower view, MS B28-B-i021, Yinkeng Formation, sample MS B28, *I. staeschei* Zone, the base of Griesbachian; 11, lateral view, MS B28-i012, Yinkeng Formation, sample MS B28, *I. staeschei* Zone, the base of Griesbachian; 12a, lateral view, MS B28-i039, 12b, lower view, MS B28-B-i039, Yinkeng Formation, sample MS B28, *I. staeschei* Zone, the base of Griesbachian.

5. *Merrillina ultima* Kozur, S_1? element, lateral view, MS B28-i029, Yinkeng Formation, sample MS B28, *I. staeschei* Zone, the base of Griesbachian.

6-7. *Merrillina ultima* Kozur, M element, 6, lateral view, MS B28-i023, Yinkeng Formation, sample MS B28, *I. staeschei* Zone, the base of Griesbachian; 7, lateral view, MS B28-i009, Yinkeng Formation, sample MS B28, *I. staeschei* Zone, the base of Griesbachian.

8, 10. *Merrillina ultima* Kozur, S_2 element, 8, lateral view, MS B28-i026, Yinkeng Formation, sample MS B28, *I. staeschei* Zone, the base of Griesbachian; 10, lateral view, MS B28-i015, Yinkeng Formation, sample MS B28, *I. staeschei* Zone, the base of Griesbachian;

Fig. 4 Conodont biostratigraphy for the Permo-Triassic boundary interval in Meishan,

Shangsi and Gaohua sections, based on Jiang et al. (2009) and Zhang et al. (2009), Jiang et al. (2011), and Wang et al., (2016), respectively.

Fig. 5 SEM photos showing *M. ultima* specimens from Shangsi and Gaohua sections

1. *Merrillina ultima* Kozur, M element, lateral view, SS-28b-i001, Feixianguan Formation, sample SS-28b, *H. changxingensis* Zone, latest Changshingian;

2. *Merrillina ultima* Kozur, P_1 element, 2a, lateral view, SS-28b-i002, 2b, lower view, SS-28b-B-i002, Feixianguan Formation, sample SS-28b, *H. changxingensis* Zone, latest Changshingian;

3. *Merrillina ultima* Kozur, $S_{3/4}$ element, lateral view, SS-28b-i003, Feixianguan Formation, sample SS-28b, *H. changxingensis* Zone, latest Changshingian.

4. *Merrillina ultima* Kozur (Fig. 3.9, Wang et al. (2016)), P_1 element, 4a, lateral view, GHC-5-i003, 4b, lower view, GHC-5-B-i003, Daye Formation, sample GHC-5, *H. parvus* Zone, the base of Griesbachian;

5. *Merrillina ultima* Kozur (Fig. 3.12, Wang et al. (2016)), P_2 element, 5a, lateral view, GHC-4-i006, 5b, lower view, GHC-5-B-i003, Daye Formation, sample GHC-4, *H. parvus* Zone, the base of Griesbachian;

6. *Merrillina ultima* Kozur, $S_{3/4}$ element, 6a, lateral view, GHC-5-i005, 6b, lower view, GHC-5-B-i005, Daye Formation, sample GHC-5, *H. parvus* Zone, the base of Griesbachian;

7. *Merrillina ultima* Kozur, $S_{3/4}$ element, 7a, lateral view, GHC-8-i001, 7b, lower view, GHC-8-B-i001, Daye Formation, sample GHC-8, *I. isarcica* Zone, the base of Griesbachian.

Fig. 6 The temporal-spatial distribution of *Merrillina*. The Meishan occurrence is from

Shen et al. (2019). *M.* sp. is from Jiang et al. (2014); *M. ultima* is from Kozur (2004); *M. postdivergens* is from Kozur (2004); transitional morphology from *M. galeata* to *M. divergens* from Clark and Behnken, 1971; *M. divergens* from Swift (1986); *M. galeata* is Wardlaw (1984). Abbreviations for the genera: *J.* for *Jinogondolella*, *C.* for *Clarkina*, *H.* for *Hindeodus*, *I.* for *Isarcicella*, *M.* for *Merrillina*.

Fig. 7 Distribution of *Merrillina* spp. from the Wordian to the Griesbachian (palaeogeography map is modified after stampfli et al., 2004). Sites: 1, Zhejiang (Meishan section), South China; 2, Hunan (Gaohua section), South China; 3, Sichuan (Shangsi section), South China; 4-6, Guizhou (4, Dawen section; 5, Zhongzhai section; 6, Dajiang section), South China; 7, Lung Cam, Vietnam; 8, Abadeh and Shahreza, Central Iran; 9, Sicily, Italy; 10, Wyoming and Nevada, United States; 11, Schleswig-Hoslstein, Germany; 12, Zechstein 1 strata, Poland; 13, Zechstein 1 strata, Northern England.

Fig. 8 Occurrence of *M. ultima* (light yellow area) compared with redox conditions in the Meishan, Shangsi, and Gaohua sections. Redox conditions are from Li et al. (2015), Bond and Wignall (2010), and Wang et al. (2016); the logs are revised in the original scale.

Table 1 Compilation of conodont abundance from the study sections (*C. yini* Zone-*I. isarcica* Zone). Data from Meishan and Shangsi are compiled from Jiang et al. (2007; 2011); Data from Gaohua are from Wang et al., 2016; *Merrillina* from this study.

Table 2 Numbers of *Merrillina* specimens recovered in study sections.

References

Bender, H., Stoppel, D., 1965. Permian-Conodonten. Geologisches Jahrbuch 82, 331-364.

Benton, M.J., 2018. Hyperthermal-driven mass extinctions: Killing models during the Permian-Triassic mass extinction. Philosophical transactions. Series A 376, 20170076.

Bond, D.P.G., Wignall, P.B., 2010. Pyrite framboid study of marine Permian–Triassic boundary sections: a complex anoxic event and its relationship to contemporaneous mass extinction. Geological Society of America Bulletin 122, 1265-1279.

Bond, D.P.G., Wignall, P.B., 2014. Large igneous provinces and mass extinctions: An update. Geological Society of America Special Papers 505, 29-55.

Bottjer, D.J., 2004. The beginning of the Mesozoic: 70 million years of environmental stress and extinction, in: Taylor, P.D. (Ed.), Extinctions in the History of Life. Cambridge University Press, Cambridge, pp. 99-118.

Brookfield, M.E., Sun, Y., 2015. Preliminary report of new conodont records from the Permian-Triassic boundary section at Guryul Ravine, Kashmir, India. Permophiles 61, 24-25.

Brosse, M., Bucher, H., Bagherpour, B., Baud, A., Frisk, A.M., Guodun, K., Goudemand, N., 2015. Conodonts from the Early Triassic Microbialite of Guangxi (South China): Implications for the definition of the base of the Triassic System. Palaeontology 58, 563-584.

Burgess, S.D., Bowring, S.A., 2015. High-precision geochronology confirms voluminous magmatism before, during, and after Earth's most severe extinction. Science Advances 1, e1500470.

Chen, J., Beatty, T.W., Henderson, C.M., Rowe, H., 2009. Conodont biostratigraphy across the Permian–Triassic boundary at the Dawen section, Great Bank of Guizhou, Guizhou Province, South China: Implications for the Late Permian extinction and correlation with Meishan. Journal of Asian Earth Sciences 36, 442–458.

Chen, L., Wang, C., 2009. Conodont-based Age of the Triassic Yangliujing Formation in SW Guizhou, China. Journal of Stratigraphy 33, 98-103.

Clark, D.L., 1972. Early Permian crisis and its bearing on Permo-Triassic taxonomy. Geologica et Paleontologica 1, 147-158.

Clark, D.L., Behnken, F.H., 1971. Conodonts and biostratigraphy of the Permian, in: Sweet, W.C., Bergström, S.M. (Eds.), Conodont Biostratigraphy, Geol. Soc. America Mem. , pp. 415-439.

Clarkson, M.O., Kasemann, S.A., Wood, R.A., Lenton, T.M., Daines, S.J., Richoz, S.,

Ohnemueller, F., Meixner, A., Poulton, S.W., Tipper, E.T., 2015. Ocean acidification and the Permo-Triassic mass extinction. Science 348, 229-232.

Fan, J., Shen, S., Erwin, D.H., Sadler, P.M., MacLeod, N., Cheng, Q., Hou, X., Yang, J., Wang, X., Wang, Y., Zhang, H., Chen, X., Li, G., Zhang, Y., Shi, Y., Yuan, D., Chen, Q., Zhang, L., Li, C., Zhao, Y., 2020. A high-resolution summary of Cambrian to Early Triassic marine invertebrate biodiversity. Science 367, 272-277.

Jiang, H., Lai, X., Luo, G., Aldridge, R., Zhang, K., Wignall, P.B., 2007. Restudy of conodont zonation and evolution across the P/T boundary at Meishan section, Changxing, Zhejiang, China. Global and Planetary Change 55, 39-55.

Jiang, H., Lai, X., Yan, C., Aldridge, R.J., Wignall, P.B., Sun, Y., 2011. Revised conodont zonation and conodont evolution across the Permian–Triassic boundary at the Shangsi section, Guangyuan, Sichuan, South China. Global and Planetary Change 77, 103-115.

Jin, Y., Shen, S., Zhu, Z., Mei, S., Wang, W., 1996. The Selong Section, candidate of Global Stratotype Section and Point of the Permian-Triassic boundary, in: Yin, H. (Ed.), The Palaeozoic-Mesozoic Boundary Candidates of the Global Stratotype Section and Point of the Permian-Triassic Boundary. China University of Geosciences Press, Wuhan, pp. 127-137.

Joachimski, M.M., Lai, X., Shen, S., Jiang, H., Luo, G., Chen, B., Chen, J., Sun, Y., 2012. Climate warming in the latest Permian and the Permian-Triassic mass extinction. Geology 40, 195-198.

Koike, T., 2016. Multielement conodont apparatuses of the Ellisonidae from Japan. Paleontological Research 20, 161-175.

Koike, T., Yamakita, S., Kadota, N., 2004. A natural assemblage of Ellisonia sp. cf. E. triassica Müller (Vertebrata: Conodonta) from the uppermost Permian in the Suzuka Mountains, central Japan. paleontological research 8, 241-253.

Kozur, H.W., 1975. Beiträge zur Conodontenfauna des Perm. Geol. Paläont. Mitt. Innsbruck 5, 1-44.

Kozur, H.W., 2004. Pelagic uppermost Permian and the Permian-Triassic boundary conodonts of Iran. Part 1: Taxonomy. Hallesches Jahrb. Geowiss. 18, 39-68.

Kozur, H.W., 2007. Biostratigraphy and event stratigraphy in Iran around the Permian-Triassic Boundary (PTB): Implications for the causes of the PTB biotic crisis. Global and Planetary Change 55, 155-176.

Li, G., Wang, Y., Shi, G.R., Liao, W., Yu, L., 2015. Fluctuations of redox conditions across the Permian–Triassic boundary—New evidence from the GSSP section in Meishan of South China. Paleogeogr. Paleoclimatol. Paleoecol. 448, 48-58.

Li, Z., Zhan, L., Dai, J., Jin, R., Zhu, X., Zhang, J., Huang, H., Xu, D., Yan, Z., Li, H., 1989. Study on the Permian-Triassic biostratigraphy and event stratigraphy of northern Sichuan and southern Shaanxi. Geological Publishing House, Beijing.

Lindström, M., 1970. A suprageneric taxonomy of the conodonts. Lethaia 3, 427-445.

Mei, S., Henderson, C.M., 2001. Evolution of Permian conodont provincilism and its significance in global corralation and paleoclimate implication. Palaeogeography, Palaeoclimatology, Palaeoecology 170, 237-260.

Metcalfe, B., Twitchett, R.J., Price-Lloyd, N., 2011. Changes in size and growth rate of 'Lilliput' animals in the earliest Triassic. Palaeogeography, Palaeoclimatology, Palaeoecology 308, 171-180.

Metcalfe, I., Nicoll, R.S., 2007. Conodont biostratigraphic control on transitional marine to non-marine Permian-Triassic boundary sequences in Yunnan-Guizhou, China. Paleogeogr. Paleoclimatol. Paleoecol. 252, 56-65.

Orchard, M.J., 2007. Conodont diversity and evolution through the latest Permian and Early Triassic upheavals. Palaeogeography, Palaeoclimatology, Palaeoecology 252, 93-117.

Orchard, M.J., Krystyn, L., 1998. Conodonts of the lowermost Triassic of Spiti, and new zonation based on Neogondolella successions. Rivista Italiana Di Paleontologia E Stratigrafia 104, 341-367.

Payne, J.L., Lehrmann, D.J., Wei, J.Y., Orchard, M.J., Schrag, D.P., Knoll, A.H., 2004. Large Perturbations of the Carbon Cycle During Recovery from the End-Permian Extinction. Science 305, 506-509.

Schobben, M., Joachimski, M.M., Korn, D., Leda, L., Korte, C., 2014. Palaeotethys seawater temperature rise and an intensified hydrological cycle following the end-Permian mass extinction. Gondwana Research 26, 675-683.

Shen, S., 2012. Meishan sections in South China: The witness of the largest biological mass extinction during the Phanerozoic. Journal of Geography 121, 570-578.

Shen, S., Cao, C., Henderson, C.M., Wang, X., Shi, G., Wang, Y., Wang, W., 2006. End-Permian mass extinction pattern in the northern peri-Gondwanan region. Palaeoworld

15, 3-30.

Shen, S., Zhang, H., Zhang, Y., Yuan, D., Chen, B., He, W., Mu, L., Lin, W., Wang, W., Chen, J., Wu, Q., Cao, C., Wang, Y., Wang, X., 2019. Permian integrative stratigraphy and timescale of China. Science China Earth Sciences 62, 154-188.

Sun, Y., Joachimski, M.M., Wignall, P.B., Yan, C., Chen, Y., Jiang, H., Wang, L., Lai, X., 2012. Lethally Hot Temperatures During the Early Triassic Greenhouse. Science 338, 366-370.

Sun, Y., Richoz, S., Krystyn, L., Grasby, S.E., Chen, Y., Banerjee, D., Joachimski, M.M., 2021. Integrated bio-chemostratigraphy of Lower and Middle Triassic marine successions at Spiti in the Indian Himalaya: Implications for the Early Triassic nutrient crisis. Global and Planetary Change 196, 103363.

Swift, A., 1986. The conodont Merrillina divergens (Bender & Stoppel) from the Upper Permian of England. Geological Society, London, Special Publications 22, 55-62.

Swift, A., Aldridge, R., 1982. Conodonts from the Upper Permian strata of Nottinghamshire and North Yorkshire. Palaeontology 25, 845-856.

Szaniawski, H., 1969. Conodonts of the Upper Permian of Poland. Acta Palaeontologica Polonica XIV, 326-342.

Wang, L., Wignall, P.B., Sun, Y., Yan, C., Zhang, Z., Lai, X., 2017. New Permian-Triassic conodont data from Selong (Tibet) and the youngest occurrence of Vjalovognathus. Journal of Asian Earth ences 146, 152-167.

Wang, L., Wignall, P.B., Wang, Y., Jiang, H., Sun, Y., Li, G., Yuan, J., Lai, X., 2016. Depositional conditions and revised age of the Permo-Triassic microbialites at Gaohua section, Cili County (Hunan Province, South China). Palaeogeography, Palaeoclimatology, Palaeoecology 443, 156-166.

Wardlaw, B.R., Collinson, J.W., 1979. Youngest Permian conodont faunas from the Great Basin and Rocky Mountain regions. Conodont biostratigraphy of the Great Basin region. Brigham Young University Geology Studies 26, 151-163.

Wardlaw, B.R., Collinson, J.W., 1984. Conodont paleoecology of the Permian Phosphoria Formation and related rocks of Wyoming and adjacent areas. Geological Society of America Special Papers 196, 263-282.

Wardlaw, B.R., Collinson, J.W., 1986. Paleontology and Deposition of the Phosphoria Formation. Contributions to Geology, University of Wyoming 24, 107-142.

Wardlaw, B.R., Mei, S., 1998. A Discussion of the early reported species of Clarkina(Permian conodonta) and the possible origin of the genus. Paleoworld 9, 33-52.

Wardlaw, B.R., Mei, S., 1999. Refined conodont biostratigraphy of the Permian and lowest Triassic of the Salt and Khizor Ranges, Pakistan, Proceedings of the International Conference on Pangea and the Paleozoic-Mesozoic transition. China University of Geosciences Press, Wuhan, pp. 154–156.

Wardlaw, B.R., Nestell, M.K., Nestell, G.P., Ellwood, B.B., Lan, L.T.P., 2015. Conodont biostratigraphy of the Permian-Triassic boundary sequence at Lung Cam, Vietnam. Micropaleontology 61, 313-334.

Wignall, P.B., Hallam, A., 1992. Anoxia as a cause of the Permian/Triassic mass extinction: facies evidence from northern Italy and the western United States. Palaeogeography, Palaeoclimatology, Palaeoecology 93, 21-46.

Xiang, L., Schoepfer, S.D., Zhang, H., Yuan, D., Cao, C., Zheng, Q., Henderson, C.M., Shen, S., 2016. Oceanic redox evolution across the end-Permian mass extinction at Shangsi, South China. Palaeogeography, Palaeoclimatology, Palaeoecology 448, 59-71.

Yan, C., Wang, L., Jiang, H., Wignall, P.B., Sun, Y., Chen, Y., Lai, X., 2013. Uppermost Permian to Lower Triassic Conodonts at Bianyang Section, Guizhou Province, South China. Palaios 28, 509-522.

Yang, W., Jiang, N., 1981. On the depositional characters and microfacies of the Changhsing Formation and the Permo–Triassic boundary in Changxing, Zhejiang. Bulletin of the Nanjing Institute of Geology and Palaeontology, Academia Sinica (in Chinese) 2, 113-133.

Yin, H., Jiang, H., Xia, W., Feng, Q., Zhang, N., Shen, J., 2014. The end-Permian regression in South China and its implication on mass extinction. Earth-Science Reviews 137, 19-33.

Yin, H., Zhang, K., Tong, J., Yang, Z., Wu, S., 2001. The Global Stratotype Section and Point (GSSP) of the Permian-Triassic Boundary. Episodes 24, 102-114.

Yuan, D., Zhang, Y., Shen, S., Henderson, C.M., Zhang, Y., Zhu, T., An, X., Feng, H., 2016. Early Permian conodonts from the Xainza area, central Lhasa Block, Tibet, and their palaeobiogeographical and palaeoclimatic implications. Journal of Systematic Palaeontology 14, 365-383.

Zhang, K., Lai, X., Ding, M., Liu, J., 1995. Conodont Sequence and its Global

Correlation of Permian-Triassic Boundary in Meishan Section, Changxing, Zhejiang Province. Earth Science-Journal of China University of Geosciences (in Chinese) 20, 669-676.

Zhang, K., Tong, J., 1996. Sequence stratigraphy of the Permian-Triassic Boundary section of Changxing, Zhejiang. Acta Geologica Sinica (in Chinese) 070, 270-281.

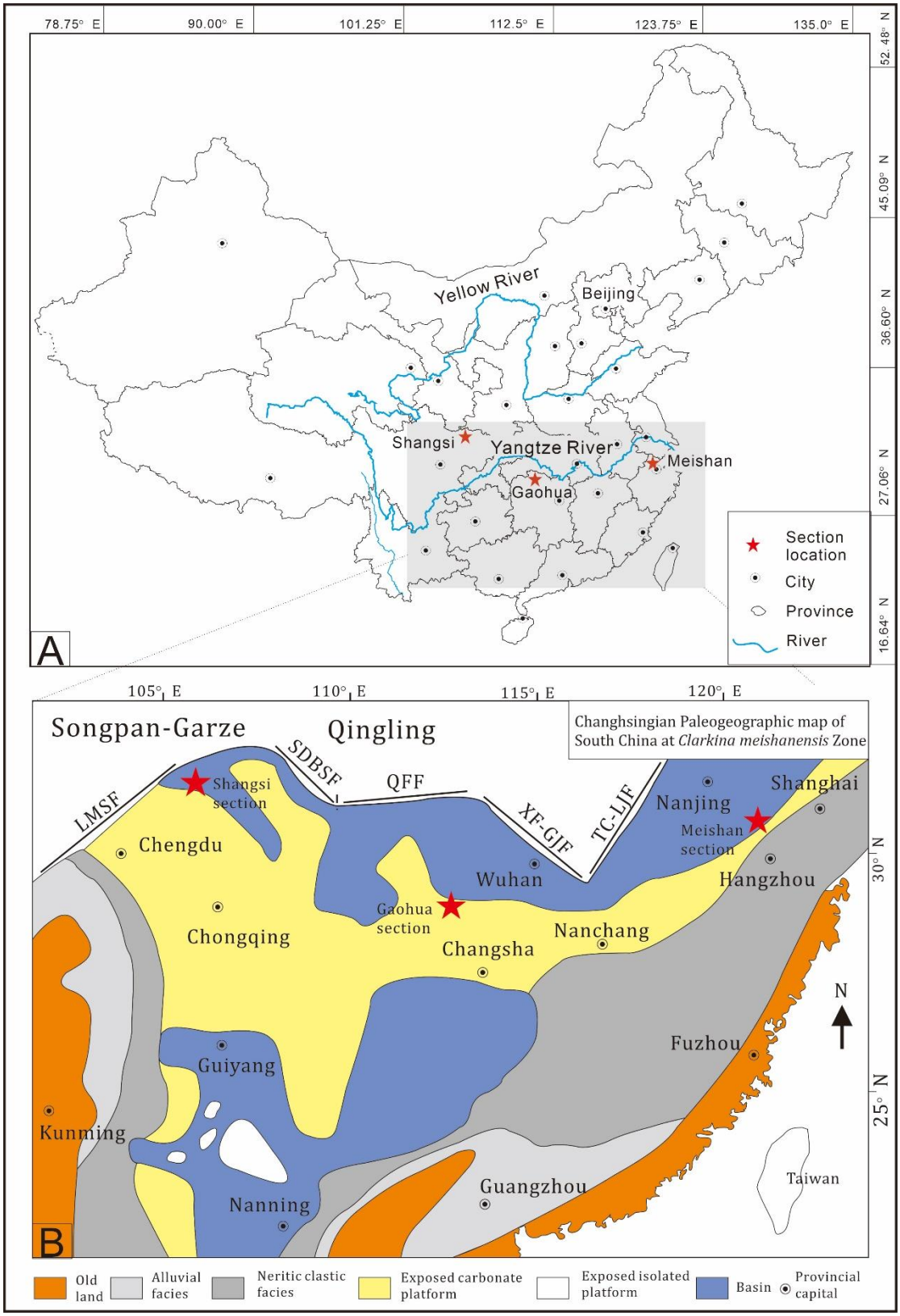
78.75° E
90.00° E
101.25° E
112.5° E
123.75° E
135.0° E
52.48° N
45.09° N
36.60° N
27.06° N
16.64° N
Yellow River
Beijing
Shangsi
Yangtze River
Meishan
Gaohua
Section location
City
Province
River
A
105° E
110° E
115° E
120° E
Songpan-Garze
Qingling
Changhsingian Paleogeographic map of South China at *Clarkina meishanensis* Zone
SDBSF
QFF
LMSF
XF-GJF
TC-LJF
Shangsi section
Chengdu
Nanjing
Shanghai
Meishan section
Hangzhou
Wuhan
Gaohua section
Chongqing
Changsha
Nanchang
N
Fuzhou
Guiyang
Kunming
Nanning
Guangzhou
Taiwan
30° N
25° N
B
Old land
Alluvial facies
Neritic clastic facies
Exposed carbonate platform
Exposed isolated platform
Basin
Provincial capital

Fig. 1

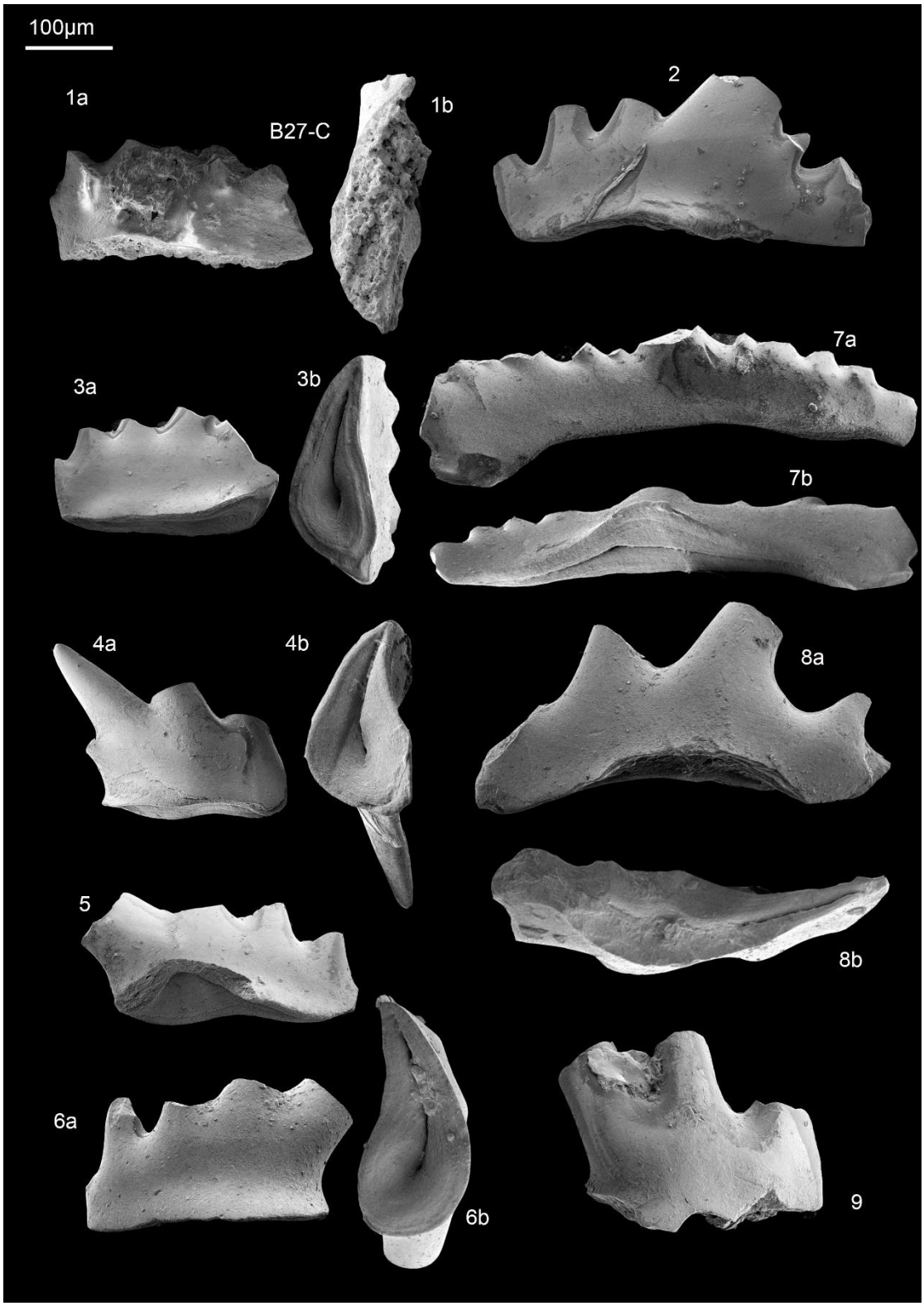

Fig. 2

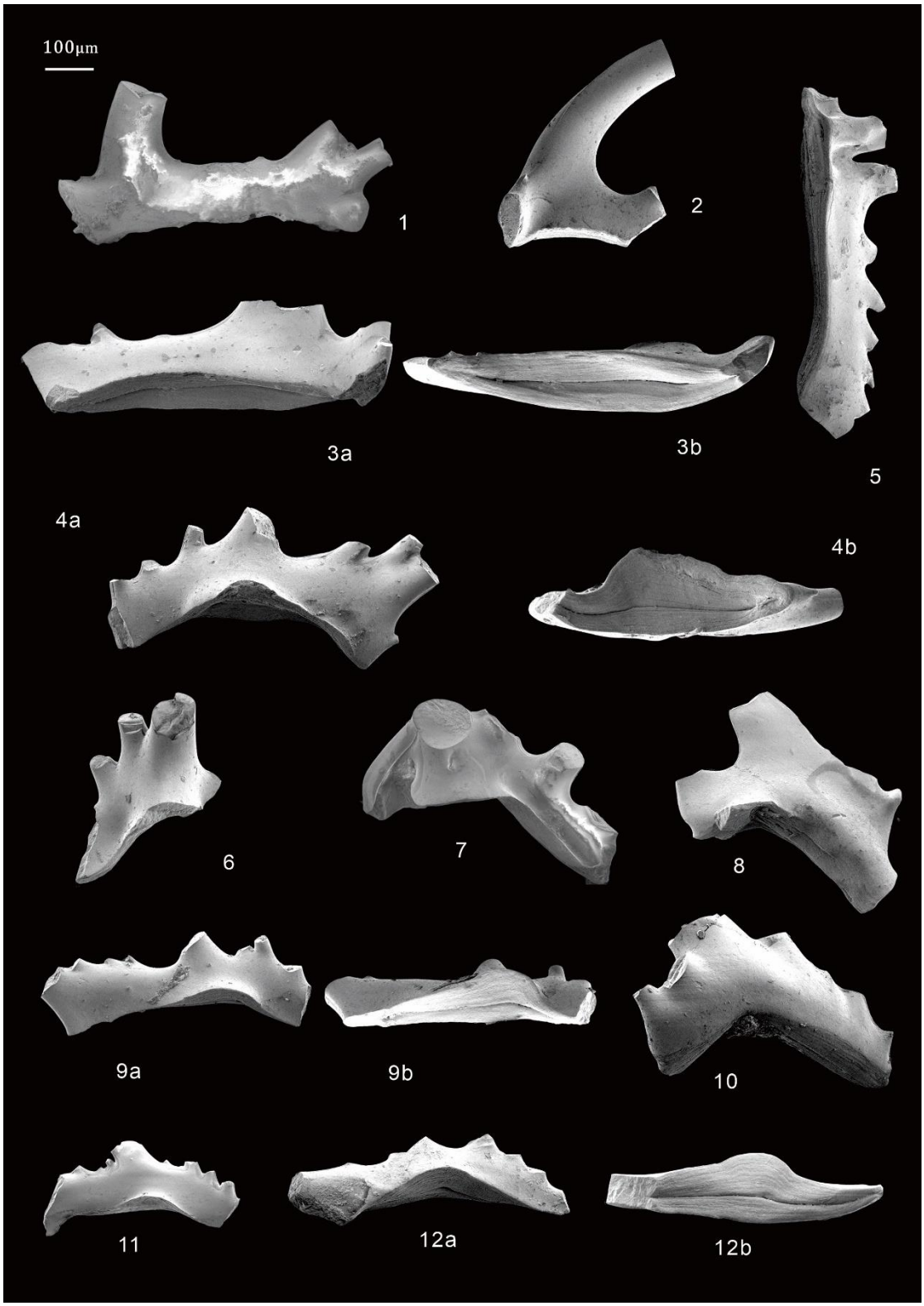

Fig. 3

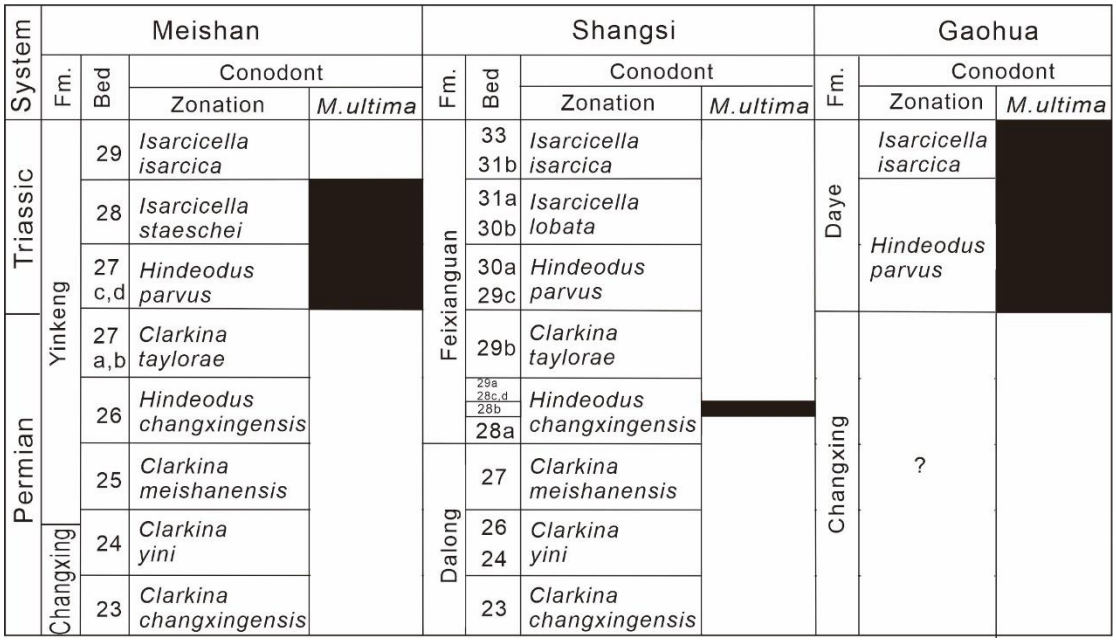
System
Meishan
Shangsi
Gaohua
Fm.
Bed
Conodont
Zonation
M.ultima
Triassic
Permian
Yinkeng
Changxing
29
28
27 c,d
27 a,b
26
25
24
23
Isarcicella isarcica
Isarcicella staeschei
Hindeodus parvus
Clarkina taylorae
Hindeodus changxingensis
Clarkina meishanensis
Clarkina yini
Clarkina changxingensis
Feixianguan
Dalong
33
31b
31a
30b
30a
29c
29b
29a
28c,d
28b
28a
27
26
24
23
Isarcicella isarcica
Isarcicella lobata
Hindeodus parvus
Clarkina taylorae
Hindeodus changxingensis
Clarkina meishanensis
Clarkina yini
Clarkina changxingensis
Daye
Changxing
Isarcicella isarcica
Hindeodus parvus
?

Fig. 4

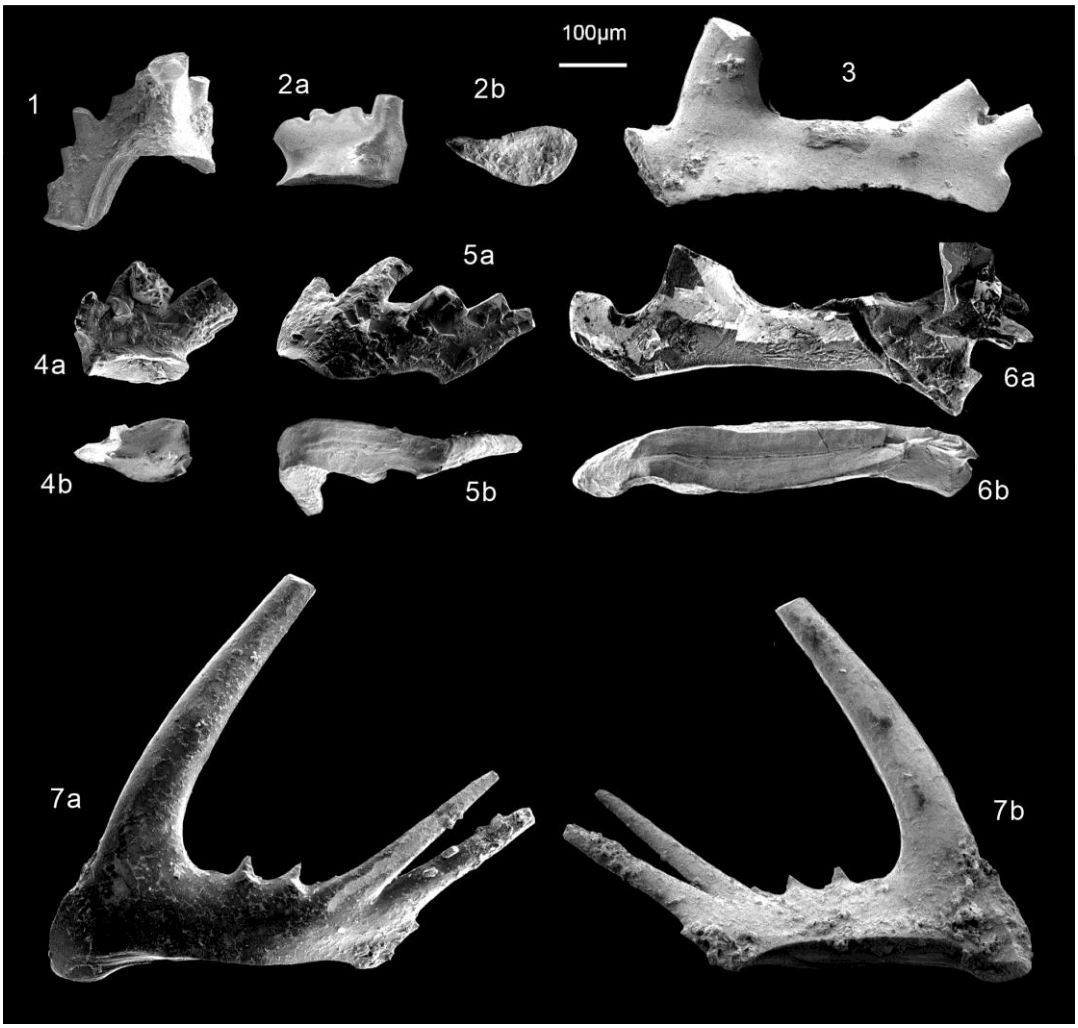
100μm
1
2a
2b
3
4a
4b
5a
5b
6a
6b
7a
7b

Fig. 5

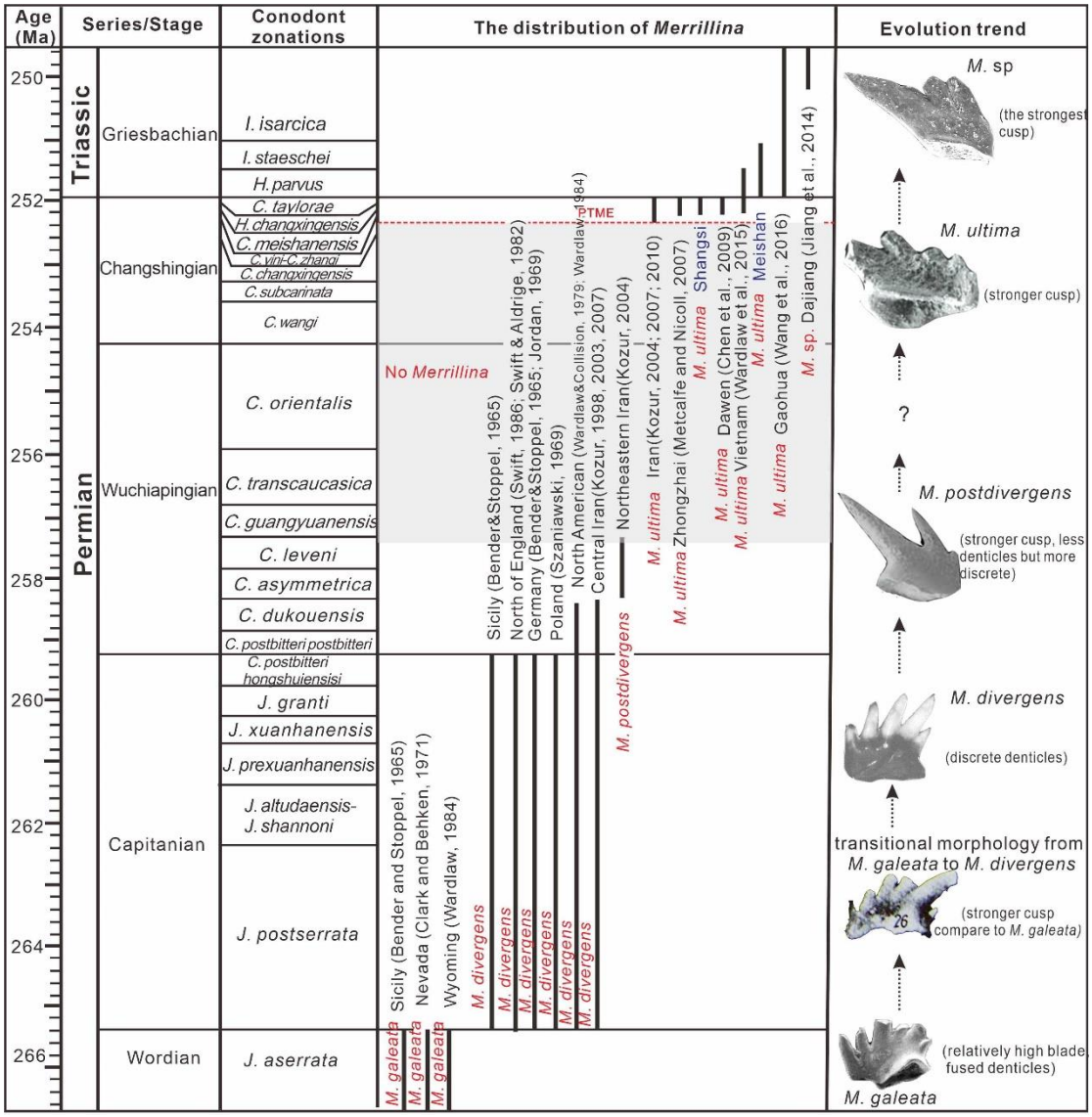
Age (Ma)
Series/Stage
Conodont zonations
The distribution of Merrillina
Evolution trend
250
252
254
256
258
260
262
264
266
Triassic
Permian
Griesbachian
Changshingian
Wuchiapingian
Capitanian
Wordian
I. isarcica
I. staeschei
H. parvus
C. taylorae
H. changxingensis
C. meishanensis
C. vini-C. zhangi
C. changxingensis
C. subcarinata
C. wangi
C. orientalis
C. transcaucasica
C. guangyuanensis
C. leveni
C. asymmetrica
C. dukouensis
C. postbitteri postbitteri
C. postbitteri hongshuiensisi
J. granti
J. xuanhanensis
J. prexuanhanensis
J. altudaensis-J. shannoni
J. postserrata
J. aserrata
TME
No Merrillina
Sicily (Bender and Stoppel, 1965)
Nevada (Clark and Behken, 1971)
Wyoming (Wardlaw, 1984)
M. galeata
M. divergens
Sicily (Bender&Stoppel, 1965)
North of England (Swift, 1986; Swift & Aldrige, 1982)
Germany (Bender&Stoppel, 1965; Jordan, 1969)
Poland (Szaniawski, 1969)
North American (Wardlaw&Collision, 1979; Wardlaw, 1984)
Central Iran(Kozur, 1998, 2003, 2007)
Northeastern Iran(Kozur, 2004)
M. postdivergens
M. ultima Iran(Kozur, 2004; 2007; 2010)
M. ultima Zhongzhai (Metcalfe and Nicoll, 2007)
M. ultima Shangsi
M. ultima Dawen (Chen et al., 2009)
M. ultima Vietnam (Wardlaw et al., 2015)
M. ultima Meishan
M. ultima Gaohua (Wang et al., 2016)
M. sp. Dajiang (Jiang et al., 2014)
M. sp
(the strongest cusp)
M. ultima
(stronger cusp)
?
M. postdivergens
(stronger cusp, less denticles but more discrete)
M. divergens
(discrete denticles)
transitional morphology from M. galeata to M. divergens
(stronger cusp compare to M. galeata)
(relatively high blade, fused denticles)
M. galeata

Fig. 6

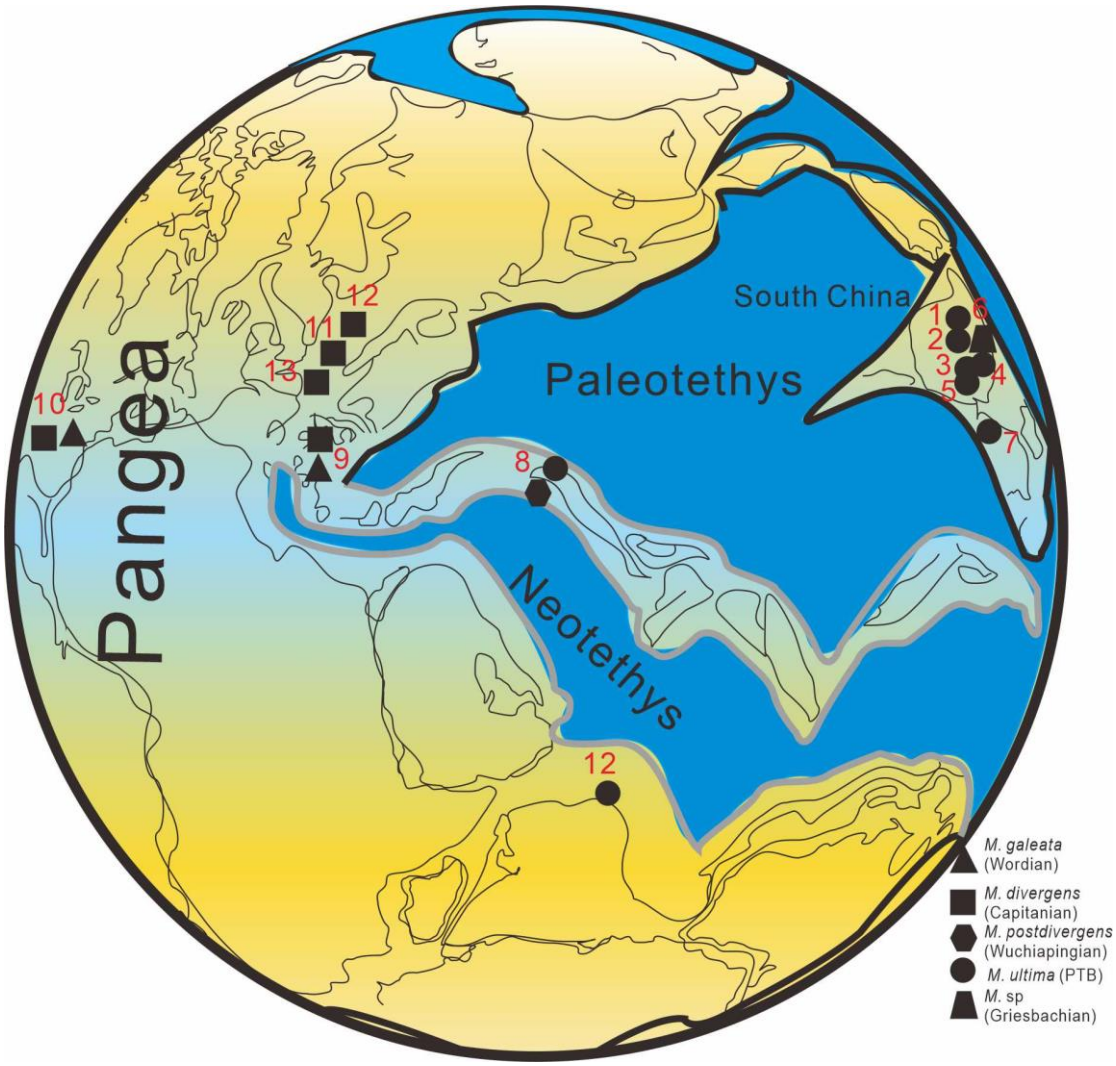
South China
Paleotethys
Pangea
Neotethys
1
2
3
4
5
6
7
8
9
10
11
12
13
12
M. galeata
(Wordian)
M. divergens
(Capitanian)
M. postdivergens
(Wuchiapingian)
M. ultima (PTB)
M. sp
(Griesbachian)

Fig. 7

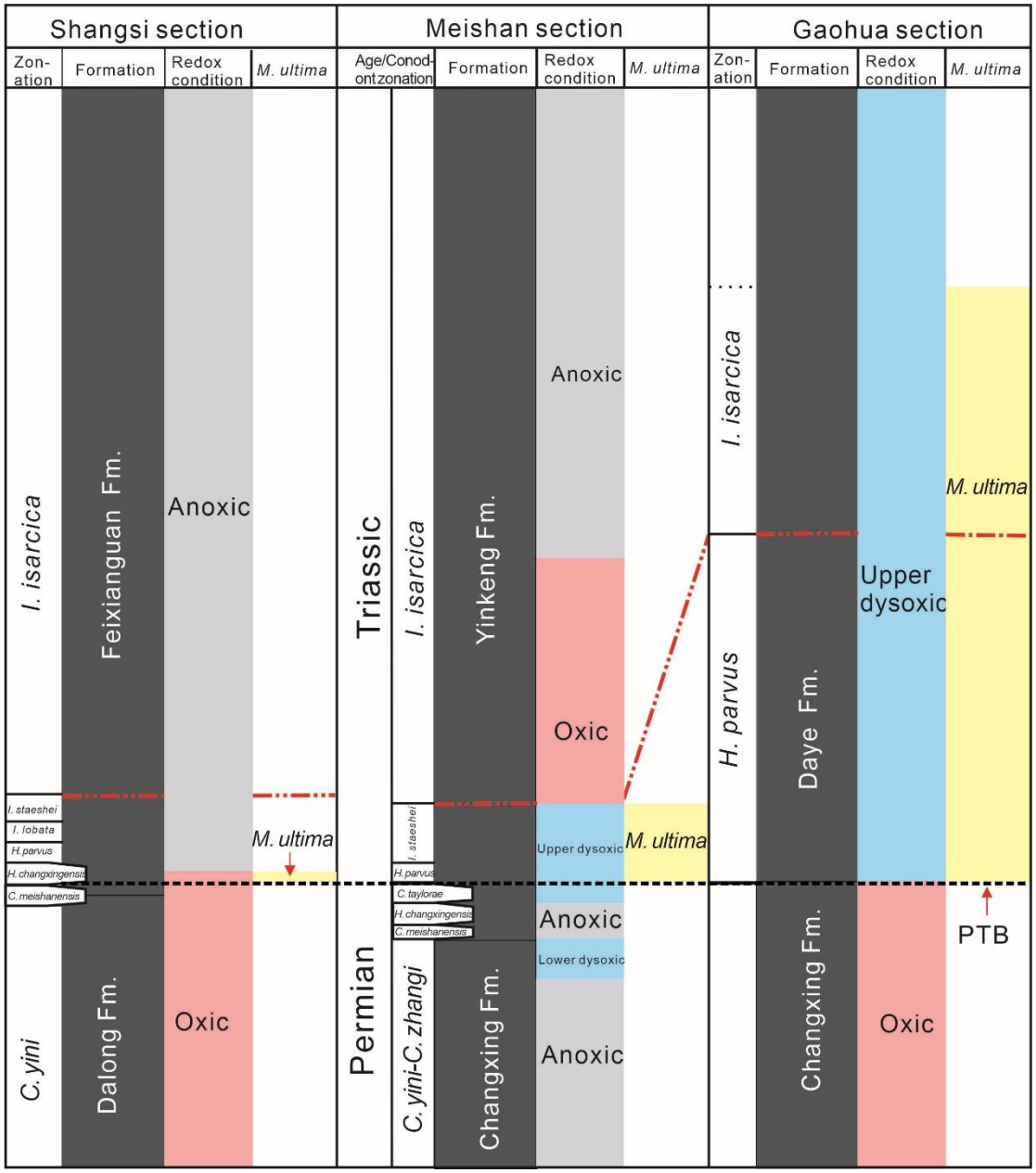
Shangsi section
Zon-ation
Formation
Redox condition
M. ultima
I. isarcica
Feixianguan Fm.
Anoxic
I. staeshei
I. lobata
H.parvus
H.changxingensis
C.meishanensis
M. ultima
C. yini
Dalong Fm.
Oxic
Meishan section
Age/Conodont zonation
Formation
Redox condition
M. ultima
Triassic
I. isarcica
Yinkeng Fm.
Anoxic
Oxic
I. staeshei
Upper dysoxic
M. ultima
H.parvus
C.taylorae
H.changxingensis
C.meishanensis
Anoxic
Lower dysoxic
Permian
C. yini-C. zhangi
Changxing Fm.
Anoxic
Gaohua section
Zon-ation
Formation
Redox condition
M. ultima
I. isarcica
H. parvus
Daye Fm.
Upper dysoxic
M. ultima
Changxing Fm.
Oxic
PTB

Fig. 8